FARADAY

Near-UV photolysis of methylamine studied by H-atom photofragment translational spectroscopy

Claire L. Reed, Mitsuhiko Kono and Michael N. R. Ashfold*†
School of Chemistry, University of Bristol, Bristol, UK BS8 1TS

H(D) atom photofragment translational spectroscopy has been used in a detailed study of the near-UV photolysis of methylamine and its deuteriated analogues at a number of wavelengths in the range 203.0–236.2 nm. Analysis of the total kinetic energy release spectra so obtained serves to reinforce recent suggestions that at least two dissociation pathways lead to H(D) atom fragments. One, 'direct', route involves N—H bond extension on the $\tilde{A}$ state surface, transfer to the ground-state surface *via* the conical intersection in the N—H exit channel and production of CH_3NH fragments carrying substantial internal excitation, behaviour very reminiscent of that exhibited by ammonia following photoexcitation to its corresponding $\tilde{A}$ excited state. Determination of the kinetic energies of the fastest H atoms formed at various of the longer excitation wavelengths yields an improved value for the N—H bond strength in methylamine: $D_0(H—NHCH_3) = 34\,550 \pm 200$ cm^{-1}. A second fragmentation channel yields H(D) atoms with a kinetic energy distribution peaking much closer to zero. Many of these are presumed to arise from the unimolecular decay of highly internally excited ground-state methylamine molecules, themselves formed *via* internal conversion from the initially prepared $\tilde{A}$ state. RRKM calculations assuming complete energy randomisation in the $CH_3NH_2^{\#}$ species prior to dissociation suggest, respectively, major and minor contributions to the total H atom yield from channels leading to the products H + CH_2NH_2 and H + CH_3NH, but the observed variations in total H(D) atom signal strength upon isotopic substitution indicate a dominant role for the N—H(D) fission process. Analyses of the measured total kinetic energy release spectra suggest that another component of the 'direct' dissociation pathway, yielding electronically excited $CH_3NH(\tilde{A})$ fragments, supplements the slow H atom yield observed at the shortest excitation wavelengths.

The first ($\tilde{A}$–$\tilde{X}$) absorption band of methylamine, CH_3NH_2, occurs in the wavelength region 190–240 nm[1–3] and has been associated with promotion of an electron from the nitrogen lone pair to an excited orbital with mixed Rydberg (3s)/antibonding valence (σ^*) character.[1,4,5] The absorption spectrum exhibits regular but diffuse vibronic structure which traditionally has been assigned in terms of progressions involving the amino wagging (ν_9) and methyl rocking (ν_{14}) vibrations.[2] This latter assignment has been called into question by recent mass resolved 1 + 1 and 2 + 2 resonance enhanced multiphoton ionisation (REMPI) studies of jet-cooled samples of the four isotopomers CH_3NH_2, CH_3ND_2, CD_3NH_2 and CD_3ND_2,[6] from which it is concluded that the second Franck–Condon active mode is better viewed as the ν_4 amine scissors vibration. The more recent analysis suggests that the geometry change upon electronic excitation is sufficiently great that the origin transition (deduced to occur at *ca.* 39 770 cm^{-1} in CH_3NH_2) has a negligible Franck–Condon factor.

Studies of methylamine photodissociation following excitation within its first absorption band are of interest for several reasons. One is the multiplicity of possible dissociation pathways. No fewer than seven fragmentation channels are energetically feasible following absorption of a 220 nm photon (*i.e.* at the wavelength corresponding to the peak of the first absorption band):

	ΔH_0/cm^{-1}	
$CH_3NH_2 + h\nu \rightarrow CH_2{=}NH + H_2$	10 600,[7]	(1)
$\rightarrow 2H_2 + HCN$	12 000,[7]	(2)
$\rightarrow CH_4 + NH$	24 900,[7]	(3)
$\rightarrow CH_3 + NH_2$	29 300,[7]	(4)
$\rightarrow CH_2NH_2 + H$	30 600,[7]	(5)
$\rightarrow CH_3NH + H$	35 900,[8]	(6)
$\rightarrow 2H_2 + HNC$	42 400.[8]	(7)

The thresholds quoted above, which are for formation of ground state products, have been derived using standard enthalpies tabulated in, or derived from, the methylamine oxidation studies of Hwang *et al.*[7] or as listed by Benson[8] and, for future reference, we note that in the case of the simple bond fissions [eqn. (4), (5) and (6)] ΔH_0 is just the bond dissociation energy D_0. As we show below, the present work indicates that Benson's estimate for the N—H bond strength [eqn. (6)] is, in fact, some 1350 cm^{-1} too high. In 1963 Michael and Noyes[9] performed a classic study of methylamine (CH_3NH_2, CH_3ND_2 and CD_3NH_2) photodissociation following broad band excitation in the wavelength range 194–244 nm, detecting H_2 formation with and without radical scavengers. As a result, they proposed a dominant (*ca.* 75%) role for the N—H bond fission [eqn. (6)] together with smaller contributions from both the C—N and C—H bond fission channels, [eqn. (4) and (5)], respectively, and the H_2 elimination pathway [eqn. (1)]. These conclusions have been largely vindicated by the more recent photofragment translational spectroscopy (PTS) studies of the 222 nm photolysis of CH_3NH_2 and CH_3ND_2.[10] Such behaviour can be compared and contrasted with that exhibited by the isoelectronic molecule CH_3OH, the UV photolysis of which is dominated by simple O—H bond fission,[11–14] and its heavier homologue CH_3SH where, again, S—H bond fission dominates, though the alternative C—S bond fission process has been shown to gain in importance with decreasing excitation wavelength.[14–18]

The near-UV photolysis of the ammonia molecule has been studied in great detail.[14,19–27] Identifying similarities and differences between its photochemistry and that of methylamine provides further justification for additional detailed study of

† E-mail: mike.ashfold@bristol.ac.uk

the latter molecule. The long-wavelength ($\tilde{A}\,^1A_2''$–$\tilde{X}\,^1A_1'$) absorption band of ammonia is dominated by a progression in the excited state out of plane (umbrella) bending mode, v_2', reflecting the change in minimum energy configuration invoked by excitation from the pyramidal (C_{3v}) ground state to the trigonal-planar (D_{3h}) $\tilde{A}\,^1A_2''$ state. Ammonia molecules in their $\tilde{A}$ state are quasi-bound; dissociation from the two lowest vibrational levels (*i.e.* those with $v_2' \leqslant 1$) occurs predominantly *via* H-atom tunnelling through a barrier in the exit channel leading to the products H + NH_2. This barrier arises as a natural consequence of Rydberg (3s) → antibonding valence (σ^*) orbital evolution as one N—H bond is extended;[19] the barrier height is least (and tunnelling consequently most facile) at planar geometries.[20,21] Recent work[27] has also highlighted another, hitherto neglected, route to these same products, *via* internal conversion to high levels of the ground state. Mass and symmetry arguments have been advanced to account for the observation that this channel makes its greatest relative contribution in the case of D-atom loss from the mixed isotopomer NHD_2. $\tilde{A}$ state ammonia molecules carrying more than one quantum of out of plane bending excitation, or excitation in vibrational modes other than v_2, have sufficient internal energy that, if redistributed appropriately, dissociation can occur by passage over (rather than through) the exit channel barrier on the $\tilde{A}$ state surface. Planarity, or otherwise, affects not just the transmission rate through (or over) this barrier, but also the asymptotic product correlations. At strictly planar geometries, the ground electronic state of ammonia correlates with the excited asymptote associated with H atoms plus electronically excited $NH_2(\tilde{A}\,^2A_1)$ products, whilst the first excited $\tilde{A}$ state of the parent correlates with the ground-state products, H + $NH_2(\tilde{X}\,^2B_1)$. Away from planarity, both the ground and the excited $\tilde{A}$ state of ammonia have the same ($^1A'$) electronic symmetry. The $\tilde{X}$ and $\tilde{A}$ state surfaces of the parent can therefore only 'cross' at planar geometries and, consequently, there is a conical intersection between these two surfaces, at planar geometries, in the H—NH_2 exit channel. As a result, the parent $\tilde{A}$ state surface shows a deep well in this exit channel, which acts as a funnel, accelerating most of the dissociating trajectories through this narrow region of configuration space onto the $\tilde{X}$ state surface and thence to the ground-state products. Indeed, energetic considerations dictate that ammonia photolysis at excitation wavelengths longer than *ca.* 206 nm can only lead to ground-state bond fission products; electronically excited H + $NH_2(\tilde{A})$ products become increasingly important in photolyses at wavelengths shorter than this, and account for *ca.* 30% of the total dissociation yield at 193 nm.[24]

This conical intersection has a profound effect on the quantum state population distributions within the resulting $NH_2(ND_2)$ fragments also. H-atom PTS experiments have shown the partner $NH_2(\tilde{X})$ fragments arising *via* this dissociation channel to be formed with little vibrational excitation, but with substantial amounts of rotational excitation, specifically distributed in the form of *a*-axis rotation. This markedly non-statistical energy disposal is a natural consequence of the conical intersection channelling (and indeed enhancing) any out-of-plane bending motion in the parent NH_3 molecule into *a*-axis rotation in the fragment.[23,24,26] These experiments also reveal that the correlation between μ, the parent transition dipole moment, and $\boldsymbol{v}$, the product recoil velocity vector (traditionally described in terms of the so called anisotropy parameter, β) is sensitively dependent upon the particular product quantum state: this, too, is understandable[26] given the topology of the parent $\tilde{A}$ and $\tilde{X}$ state potential-energy surfaces and the constraints imposed by energy and angular momentum conservation.

Kassab *et al.*[4] and, recently, Dunn and Morokuma[5] have reported cuts through *ab initio* potential-energy surfaces for the $\tilde{A}$ and $\tilde{X}$ states of methylamine. These show that the $\tilde{A}$ state potential for both N—H and C—N bond fission pathways [channels (6) and (4), respectively] is, in each case, characterised by a small barrier at short range and, at larger separations, by a conical intersection with the ground-state surface at geometries for which the NH_2 moiety, the C atom and one of the methyl H atoms are coplanar. The topology of the $\tilde{A}$ and $\tilde{X}$ state surfaces along the N—H dissociation coordinate in methylamine appears, qualitatively, very similar to that in ammonia. Dunn and Morokuma[5] suggest a long-wavelength threshold of *ca.* 210 nm for dissociation to an H atom plus an electronically excited $CH_3NH(^2A')$ fragment. They also calculate that the barrier to C—N bond fission on the excited-state surface is somewhat larger than that for dissociation *via* N—H bond cleavage, a fact that is perhaps relevant in explaining the predominance of the latter dissociation channel following UV excitation of CH_3NH_2. The C—H bond stretching coordinate, in contrast, shows no avoided crossing with the ground-state surface.[5] The parent $\tilde{A}$ state surface correlates adiabatically with an H atom and an electronically excited CH_2NH_2 fragment; the long-wavelength threshold for this process is calculated to be at *ca.* 190 nm. Thus any experimentally observed products attributable to dissociation channel (5) must arise as a result of internal conversion from the initially populated $\tilde{A}$ state and subsequent dissociation on the ground-state surface. Such is broadly consistent with the experimental observations reported to date:[10] the total kinetic energy release (TKER) spectra associated with the H + CH_3NH and CH_3 + NH_2 product channels both peak away from zero kinetic energy, consistent with dissociation on a surface for which there is a barrier to the reverse reaction, whilst the TKER spectrum attributed to the H + CH_2NH_2 channel is deduced to peak near zero.

Here we report high-resolution TKER spectra of the H(D) atom photofragments arising in the photodissociation of the four isotopomers CH_3NH_2, CH_3ND_2, CD_3NH_2 and CD_3ND_2 following excitation at many different wavelengths in the range 203.0–236.2 nm. The general forms of these spectra accord with the earlier results from Butler's group[10] and are interpreted in terms of contributions both from direct bond fission processes and from slower, more 'statistical' unimolecular decays. The density of product states precludes observation even of product vibrational structure in the TKER spectra save for those recorded at the longest excitation wavelengths; from these it is possible to extract an improved estimate of the N—H bond strength in methylamine. TKER spectra recorded for the various isotopomers of methylamine are quantitatively similar to those for CH_3NH_2, though the weakness of the H atom signal from CH_3ND_2 photolysis and of the D atom signal from CD_3NH_2 serves to reinforce previous conclusions[9] regarding the relative importances of N—H and C—H bond fission channels in the UV photodissociation of methylamine. The remainder of this paper attempts to place our results in the context of previous knowledge concerning the UV photochemistry of this molecule.

Experimental

The apparatus used to measure H-atom photofragment translational spectra and the 'tagging' of the H atoms has been described previously.[17,28–30] Briefly, a molecular beam of the parent molecule of interest is prepared by passing a mixture of methylamine in Ar (typical mixing ratio 5–15%, total stagnation pressure *ca.* 1 atm.) through a pulsed nozzle (General Valve Series 9) and a skimmer into a second chamber, differentially pumped by a cryopump (APD-Cryogenics). The molecules are first photolysed by the output of one laser (in the wavelength range 203.0–236.2 nm) which intercepts the molecular beam at right angles, downstream from the skimmer. The

resulting H atom photofragments are then 'tagged' *via* a two-colour, two-photon excitation to a high-n Rydberg state. The photolysis and tagging laser systems have all been detailed previously.[17] The photolysis wavelengths used in the present work were obtained using the dyes sulfurhodamine 640, DCM or LDS-698, and first doubling (in KDP) and then mixing the resulting ω and 2ω frequencies (in BBO). The 3ω radiation so derived was linearly polarised, with its electric vector aligned perpendicular to the TOF axis. The detected H (or D) atoms fly a field-free distance of 425 mm (825 mm in the case of H-atom TOF spectra recorded from CH_3NH_2 photolysis at 203 and 210 nm) along the third orthogonal axis and are ionised immediately prior to detection by a Johnston multiplier (type MM1-SG). The output from the multiplier is amplified and sent to one channel of a digital storage oscilloscope (LeCroy 9450, 350 MHz bandwidth) for display. This transient TOF spectrum is transferred to a computer (IBM PS-2) *via* a GPIB interface and the spectrum is allowed to accumulate over typically 10^4 laser shots. Energy and momentum conservation allows conversion of the accumulated TOF spectra to total kinetic energy release spectra as described in previous publications.[17,28–30]

CH_3NH_2 (Cambrian Gases) and argon carrier gas (BOC) were obtained commercially and used as supplied. Fully and partially deuteriated methylamines were obtained from Aldrich, Inc. as the salts $CD_3NH_2 \cdot HCl$, $CH_3ND_2 \cdot DCl$ and $CD_3ND_2 \cdot DCl$ and prepared according to the method of Tsuboi *et al.*[2] and Taylor and Bernstein.[6] The samples were placed with frozen sodium hydroxide in an evacuated glass flask and heated slowly. We found this procedure to work well for CD_3NH_2, which was then trapped with liquid nitrogen. Reliable preparation of CH_3ND_2 and CD_3ND_2 from reaction of the appropriate salt with NaOD (itself prepared by addition of pellets of sodium metal to a minimum quantity of D_2O) proved more challenging, even though the solution volume of NaOD was kept to a minimum. In each case we observed that the reaction starts as soon as the sodium hydroxide begins to melt; only very gentle heating was thus required. The purity of each isotopomer was assessed by UV absorption spectroscopy. As a further check, a sample of CH_3NH_2 was prepared using the equivalent reaction (of $CH_3NH_2 \cdot HCl$ with NaOH). Photolysis yielded H-atom TOF spectra identical to those obtained using the lecture bottle sample. D_2O vapour was pulsed through the nozzle prior to experiments involving CH_3ND_2 and CD_3ND_2, in an attempt to minimise subsequent D/H isotopic exchange.

Results

Fig. 1 shows H-atom TOF spectra resulting from photolysis of jet-cooled samples of CH_3NH_2 at six wavelengths in the range 236.2–203.0 nm. None of these spectra show much fine structure, though each is characterised by a 'tail' extending to long times, indicative of some branching into fragments with little translational (and consequently high internal) energy. If we attribute the entire H-atom signal in such TOF spectra to dissociation channels (5) and/or (6), then any given TOF, t_H, may be converted to the corresponding TKER (assuming conservation of total energy and linear momentum) *via* the relationship:

$$E_{kin,\,total} = E_{kin,\,H} + E_{kin,\,CH_4N} = \frac{1}{2} m_H \left(1 + \frac{m_H}{m_{CH_4N}}\right)\left(\frac{d}{t_H}\right)^2 \quad \text{(I)}$$

Fig. 2 and 3 show the corresponding TKER spectra (plotted from upwards of 1500 cm^{-1}) for the H + CH_4N products resulting from CH_3NH_2 photolysis at these six wavelengths. Spectra obtained at the longer excitation wavelengths (Fig. 2) each show reasonably clear onsets at high kinetic energy, and one or more partially resolved steps, but most of the signal

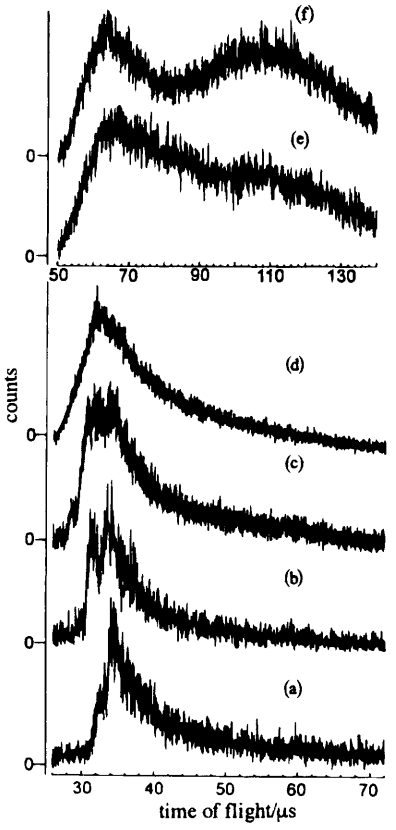

Fig. 1 H-atom TOF spectra obtained following linearly polarised photolysis of a jet-cooled sample of CH_3NH_2 molecules at (a) 236.2, (b) 233.3, (c) 225.4, (d) 219.0, (e) 210.0 and (f) 203.0 nm with, in each case, ε_{phot} aligned perpendicular to the flight axis. The larger TOFs in (e) and (f) are due to the use of our longer (825 mm) flight path when recording these particular spectra.

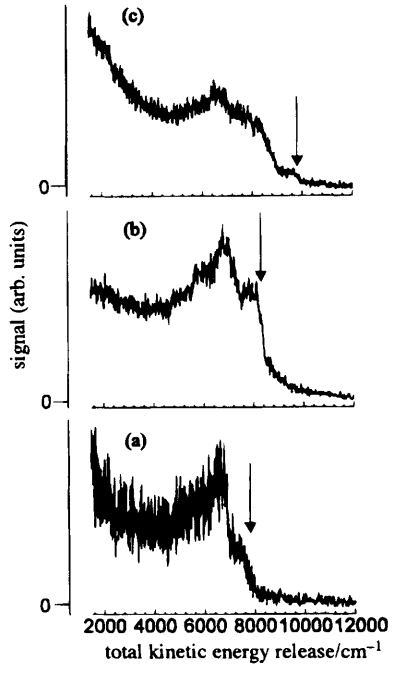

Fig. 2 TKER spectra (derived assuming that the partner fragment to all of the observed H atoms has a mass of 30 u) resulting from photolysis of jet-cooled CH_3NH_2 molecules at 236.2 (42 326), (b) 233.3 (42 854) and (c) 225.4 nm (44 357 cm^{-1}). The vertical arrows indicate the maximum TKER allowed by energy conservation.

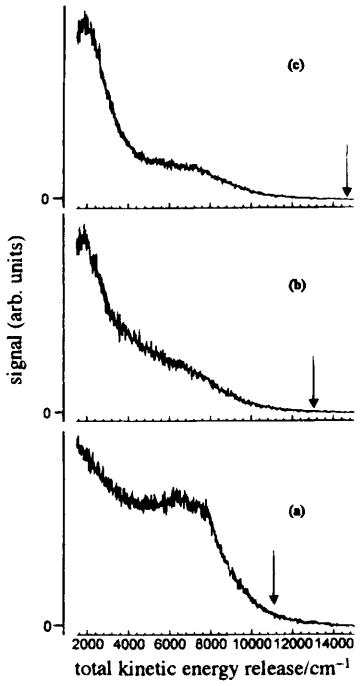

Fig. 3 TKER spectra (again derived assuming that CH_4N fragments partner all of the observed H atoms) resulting from photolysis of jet-cooled CH_3NH_2 molecules at (*a*) 219.0 (45 648), (*b*) 210.0 (47 605) and (*c*) 203.0 nm (49 245 cm^{-1}). The vertical arrows indicate the maximum TKER allowed by energy conservation.

resulting from photolysis at the shorter excitation wavelengths lies at much smaller kinetic energy releases, implying substantial excitation of internal degrees of freedom of the CH_4N partner. Such behaviour is very reminiscent of that exhibited by ammonia following photodissociation within its $\tilde{A}$–$\tilde{X}$ absorption band.[24,26]

Before proceeding further it is important to establish, as far as is possible, that the entire TOF signal is attributable to primary photolysis products. Fig. 4 shows TKER spectra (derived assuming that the partner fragment to all of the observed H atoms has chemical formula CH_4N and a mass of 30 u) obtained from CH_3NH_2 photolysis at 230.6 nm, using pulse energies of (a) 0.7 mJ and (b) 2.0 mJ per pulse. The spectra appear identical, encouraging the assumption that

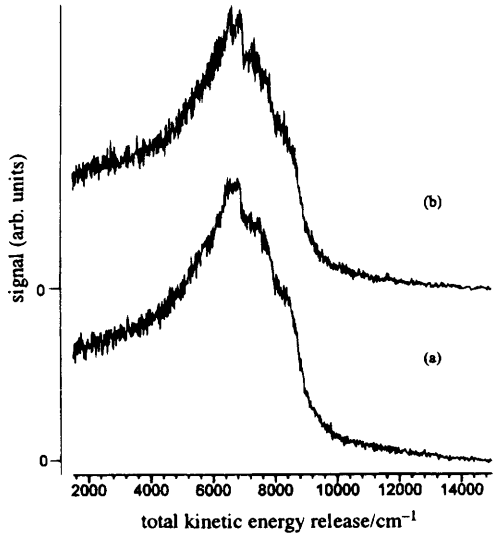

Fig. 4 TKER spectra (again derived assuming that the partner fragment to all of the observed H atoms has mass 30 u) obtained from CH_3NH_2 photolysis at 230.6 nm, using pulse energies of (a) 0.7 and (b) 2.0 mJ per pulse.

under the present experimental conditions secondary photolyses of, for example, CH_4N fragments arising *via* channels (5) or (6), or CH_3 or NH_2 fragments formed *via* the dissociation (4), make negligible contribution to the measured H atom yield. We also tested to ensure that the forms of the measured H-atom TOF spectra were independent of the CH_3NH_2/Ar mixing ratio in the molecular beam source, thereby eliminating the possibility that any significant part of the measured spectra resulted from photolysis of cluster species.

The onsets indicated in Fig. 2 are all consistent with a value of 34 550 ± 200 cm^{-1} for the threshold energy for forming H atoms: both dynamic and thermodynamic considerations, and all past estimates of the various branching ratios for fragmentation channels (1)–(7), lead us to associate this threshold with D_0(H—$NHCH_3$). This value is some 1350 cm^{-1} lower than Benson's earlier estimate of this bond strength,[8] and some 2500 cm^{-1} lower than the corresponding N—H bond strength in NH_3. Similar, though less dramatic, reductions have been noted in the O—H and S—H bond strengths upon going from H_2O to CH_3OH[31] and from H_2S to CH_3SH,[17,32] respectively. We presume all of these observations to be explicable in terms of the weak electron donating effect of the methyl moiety introducing some antibonding character into the neighbouring (dissociating) X—H bond.

Fig. 5 shows TKER spectra monitored *via* the H(D) atom for 225.4 nm (44 357 cm^{-1}) photolysis of four isotopomers of methylamine. The thresholds at high TKER in the spectra from CH_3NH_2 and CD_3NH_2 photolysis are consistent with, in each case, fission of an N—H bond. The corresponding thresholds in the spectra from CH_3ND_2 and CD_3ND_2 are less obvious but, as shown in Fig. 5(c) and (d), may just be discernible some 1200 cm^{-1} to higher kinetic energy release. Such a variation in bond strength would be consistent with the known differences in zero-point energy on substituting an

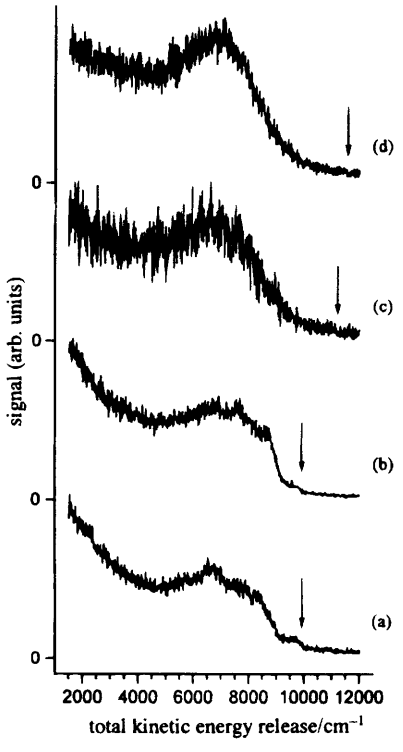

Fig. 5 TKER spectra obtained following 225.4 nm photoexcitation of various isotopomers of methylamine: (a) and (b) involved monitoring the H atoms resulting from photolysis of, respectively, CH_3NH_2 and CD_3NH_2, whereas (c) and (d) were obtained by detecting D atoms from photolysis of CH_3ND_2 and CD_3ND_2 respectively. The vertical arrows indicate the deduced maximum total kinetic energy releases.

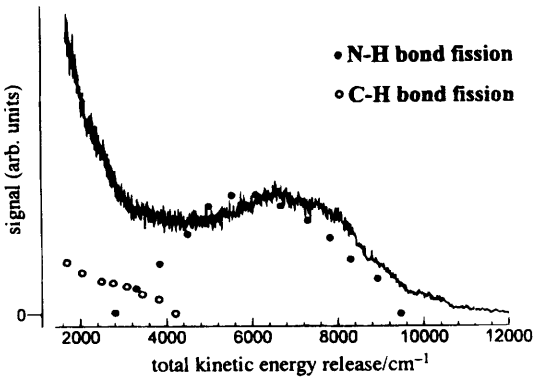

Fig. 6 TKER spectra obtained by monitoring the H photofragments resulting from 222.0 nm photolysis of CH_3NH_2 together with (open and filled circles) the results of one earlier study of this photolysis.[10] The two data sets have been plotted so that the fast part of the signal has the same peak intensity in each case.

ND_2 group in place of the NH_2 moiety. However, we should mention at this stage that we always observed some H-atom fragments when photolysing what was, nominally, a CH_3ND_2 sample, and, similarly, some D fragments when exciting CD_3NH_2. This could point to a role for C—H(C—D) bond fission but, as we argue in more detail below, the fact that these alternative products show very similar TKER spectra to those of the more abundant D(H) fragment leads us to suspect that the minor product arises largely as a result of our inability to prepare 100% pure samples of the mixed isotopomers CH_3ND_2 and CD_3NH_2.

Finally, in Fig. 6, we compare the TKER spectra obtained by monitoring the H photofragments resulting from 222.0 nm photolysis of CH_3NH_2 with that reported in the earlier work of Waschewsky *et al.*[10] The high kinetic energy parts of the two spectra are reassuringly similar, but the present experiments indicate a significantly larger fraction of slow H atoms than deduced hitherto.

Discussion

The TOF data obtained in the PTS experiments of Butler and co-workers,[10] involving isotopic variants of CH_3NH_2 and mass spectrometric detection of the nascent fragments, has been interpreted by assuming that the N—H, C—H and C—N bond fissions [channels (6), (5) and (4), respectively] and the H_2 molecular elimination channel (1) all contribute to the primary UV photochemistry of methylamine. The present work is, of course, only sensitive to dissociation channels yielding an H atom [*i.e.* channels (5) and (6)] and from hereon attention is focused largely on these two primary processes. As discussed earlier, the *ab initio* calculations of Dunn and Morokuma[5] show the N—H dissociation coordinate on the $\tilde{A}$ state surface to involve, first, a small potential barrier at short R_{N-H} bond extensions and, at larger R, a conical intersection with the ground-state surface at geometries for which the C—N bond, the NH_2 moiety and one of the methyl C—H bonds are coplanar. These calculations also suggest a value of *ca.* 210 nm for the wavelength corresponding to the energetic threshold for forming electronically excited $CH_3NH(\tilde{A})$ fragments. Thus, for all but the shortest wavelengths investigated here, ground-state CH_3NH fragments are the only thermodynamically allowed products arising from the N—H bond fission process. As in ammonia, the effect of this conical intersection will be to channel any out-of-plane motion in the excited parent molecule into fragment internal (particularly rotational) excitation. Such an expectation is consistent with the experimental observations: (*i*) the TKER spectra obtained at the longest excitation wavelengths (Fig. 2) indicate some formation of $CH_3NH(\tilde{X})$ fragments with no internal excitation, but the vast majority are formed with $E_{int} \gg 0$, (*ii*) the separations (*ca.* 900 cm^{-1}) of the 'steps' apparent in the TKER spectra recorded at the longer excitation wavelengths are sensibly consistent with that expected for the in-plane HNC bending vibration in the CH_3NH fragment[34] which, on Franck–Condon grounds and by analogy with NH_3 photolysis,[24,26] might well be expected to be active during the dissociation process, and (*iii*) the fraction of internally 'cold' fragments declines as the excitation wavelength is reduced (see, for example, Fig. 3). All of these observations mimic trends noted previously in the case of the UV photolysis of ammonia.[24]

The various TKER spectra reported here (*e.g.* Fig. 2 and 3) and previously (Fig. 6) all show a bimodal kinetic energy distribution with a second maximum peaking at low kinetic energies. Butler and co-workers[10] attributed these slow H atoms to dissociation pathway (5), occurring after internal conversion (IC) to high levels of the ground electronic state. We concur with the view that many of these slow H atoms arise from unimolecular decay of internally 'hot' ground-state molecules (henceforth identified as $CH_3NH_2^{\#}$), but now proceed to explore their attribution to pathways (5) or (6) in a little more detail. Fig. 7 shows the form of the TKER spectra that we might expect for the H + CH_3NH and H + CH_2NH_2 products resulting from CH_3NH_2 photolysis at 222.0 nm if we assume (*i*) complete energy randomisation in the $CH_3NH_2^{\#}$ molecules, and (*ii*) that the probability of forming fragment pairs with any particular total kinetic energy, E, is thus simply proportional to the total density of product states, ρ_{tot}, at that energy. The calculation of the respective $\rho(E)$ functions followed closely that described in our earlier modelling of the unimolecular decay of the $CH_4^{\#}$ molecules arising in the 121.6 nm photoexcitation of methane,[29] *i.e.* $\rho(E)$ is treated as the product of the vibrational state density $N(E_v)$ in the $CH_3NH(CH_2NH_2)$ fragment at each energy above the appropriate dissociation threshold, multiplied by a term $(E_{kin})^{1/2}$ to allow for the three-dimensional translational density of states of the recoiling fragments. For the present purposes it is sufficient to calculate $N(E_v)$ using the Whitten–Rabinovitch approximation[33]

$$N(E_v) = \frac{(E_v + aE_z)^{s-1}}{(s-1)!\,\Pi h\nu_i} \qquad \text{(II)}$$

where, following convention, E_v is the fragment vibrational energy measured from the zero-point level and E_z is the zero-point energy (both calculated assuming the harmonic normal mode frequencies listed in Table 1) and s is the number of

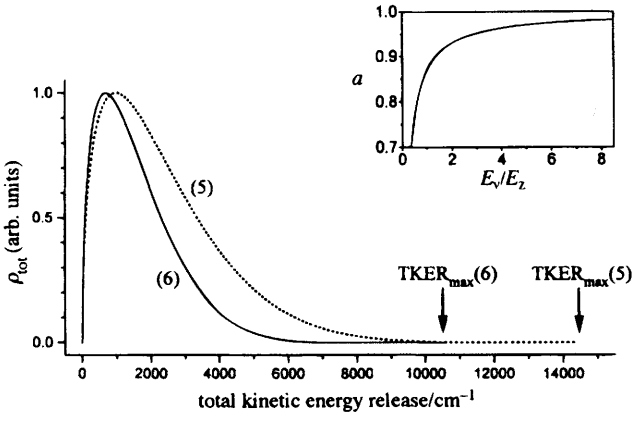

Fig. 7 Calculated form of the total density of states, $\rho(E)$, associated with the H + CH_2NH_2 [channel (5)] and H + CH_3NH [channel (6)] products resulting from CH_3NH_2 photolysis at 222.0 nm assuming complete energy randomisation in the $CH_3NH_2^{\#}$ molecules. The inset shows the energy dependence assumed for the a parameter in eqn. (II).

Table 1 Normal-mode vibrational frequencies of CH_3NH_2, CH_3NH and CH_2NH_2 used in the density of states calculations reported here

	normal mode frequencies/cm^{-1}
CH_3NH_2 [6,34]	3361, 2961, 2820, 1623, 1473, 1430, 1130, 1044, 780, 3427, 2985, 1485,[a] 1455,[a] 1195,[a] 268
CH_3NH [35 b]	3293, 2924, 2826, 1450, 1402, 1292, 1018, 964, 2867, 1460, 966, 266
CH_2NH_2 [35 b]	3398, 2941, 1629, 1439, 1122, 782, 677, 3483, 3038, 1301, 916, 390

[a] Not directly observed. [b] All reduced by 10% *cf.* the values reported in ref. 35, in recognition of the fact that such SCF calculations traditionally overestimate the real frequencies.

vibrational modes (12 in the present case). The assumed energy dependence of the parameter a is shown in the inset to Fig. 7. Rotational excitation is ignored in all of these calculations. Both calculated distributions have a general form that, qualitatively at least, appears consistent with the slow part of the observed TKER spectra.

Thus it is tempting to attempt to partition the observed TKER spectra in terms of a 'direct' or 'dynamical' component (associated with dissociation on the $\tilde{A}$ state surface and coupling *via* the conical intersection to the H + CH_3NH asymptote) and a 'statistical' component resulting from unimolecular decay of $CH_3NH_2^{\#}$ molecules. Fig. 8 illustrates such decompositions for the case of TKER spectra obtained following excitation of CH_3NH_2 at 225.4, 219.0 and 203.0 nm. For simplicity, the 'statistical' contribution was calculated

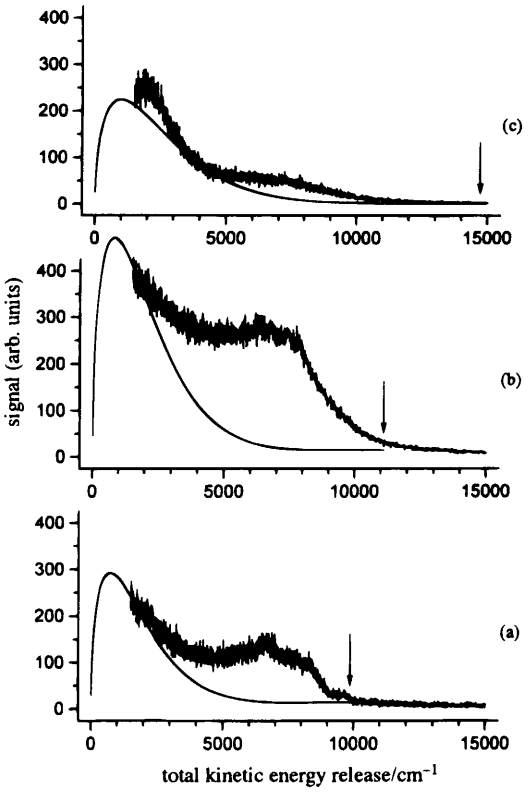

Fig. 8 Model partitioning of the TKER spectra observed following excitation at (a) 225.4, (b) 219.0 and (c) 203.0 nm. The vertical arrows indicate the maximum total kinetic energy release at each excitation wavelength, assuming contribution from the N—H bond fission channel only. The smooth curves in (a) and (b) show the result of least squares fitting to the 1500–2000 cm^{-1} part of the respective TKER spectra, assuming a 'statistical' energy partitioning involving N—H bond fission only. No comparable fit is possible for the data displayed in (c) but, for illustration, we show the calculated curve that results if we assume a 'statistical' energy partitioning (again involving N—H bond fission only) and fit to the 3500–4000 cm^{-1} part of the data. Dissociation yielding electronically excited $CH_3NH(\tilde{A})$ fragments is proposed to account for the surfeit of slower H atoms.

assuming involvement of the N—H bond fission process only. The relative weightings of the 'direct' and 'statistical' contributions were determined by least-squares fitting to that part of each experimental TKER spectrum deemed to be least contaminated by contributions from the 'direct' channel (*i.e.* the 1500–2000 cm^{-1} portion for spectra resulting from excitation at 225.4 and 219.0 nm and the 3500–4000 cm^{-1} portion for excitation at 203.0 nm). Such an analysis suggests that both fragmentation routes make comparable contributions to the total H atom yield following excitation at wavelengths longer than *ca.* 215 nm, but a more precise estimate of this branching would require TKER spectra displaying a better signal-to-noise ratio, and taken at more than one photolysis laser polarisation to confirm the small angular anisotropy reported by Waschewsky *et al.*[10] (following photolysis at 222 nm) and that β was insensitive to the product kinetic energy. The fit to TKER spectra recorded at shorter excitation wavelengths is noticeably poorer. Consider the TKER spectrum obtained at 203.0 nm [Fig. 8(c)]. The 'slow' part of the TKER spectrum rises more sharply and peaks at larger TKER than would be predicted by any statistical model. One plausible interpretation for the dominant slow peak observed following excitation at 203.0 nm and, to a lesser extent, at 210.0 nm [recall Fig. 3(b)], is dissociation yielding electronically excited $CH_3NH(\tilde{A})$ fragments. Analogy with ammonia[24,36] suggests that such a process, involving dissociation on the parent $\tilde{A}$ state surface, should occur. Unfortunately we can find no experimental reports of the $\tilde{A}$–$\tilde{X}$ band system of CH_3NH, but an adiabatic energy separation of *ca.* 10000 cm^{-1} (similar to the $\tilde{A}$–$\tilde{X}$ separation in the NH_2 radical) would fit the present data well, and accords with theoretical prediction.[5] As in the near-UV photolysis of NH_3 [36] we would expect these $CH_3NH(\tilde{A})$ fragments to carry a broad spread of internal energies, consistent with the absence of any sharp step in the slow part of the present TKER spectra.

Finally, we return to the question as to which of channels (5) or (6) provides the major contribution to the yield of slow H atoms arising *via* the 'statistical' fragmentation pathway. If we assume complete energy randomisation in the $CH_3NH_2^{\#}$ molecules formed as a result of IC from the initially excited $\tilde{A}$ state, then RRKM theory should provide a reasonable estimate of the energy-dependent rate constant, $k(E)$, for unimolecular decay *via* the bond fission processes (5) and (6). This can be estimated, for each of the two dissociation paths and for each excess energy ($E - D_0$), *via* the standard expression (III):[33,37]

$$k(E) = \frac{\sum_{E=D_0}^{E} P(E - D_0)}{hN(E)} \qquad \text{(III)}$$

where the numerator represents the number of vibrational states in the respective transition states with energy $E > D_0$ and $N(E)$ is the vibrational state density of the parent CH_3NH_2 molecule at internal energy E. The respective sum of states terms for the transition states leading to N—H and C—H bond fission were also calculated using the Whitten–Rabinovitch approximation, *i.e.*

$$\sum_{E_v=0}^{E_v} P(E_v) = \frac{(E_v + aE_z)^s}{s! \prod h\nu_i} \qquad \text{(IV)}$$

where E_v and E_z have their traditional meanings, a is parametrised as in the inset to Fig. 7 and, in this case, $s = 14$, together with the following bond strengths: $D_0(H{-}NHCH_3) = 34\,550\ cm^{-1}$ (derived in the present work) and $D_0(H{-}CH_2NH_2) = 30\,600\ cm^{-1}$ from Hwang *et al.*[7] In both cases we assume that 12 of the normal mode vibrational frequencies remain as in the parent CH_3NH_2 molecule (see Table 1). For the former transition state, the NH_2 asymmetric stretching mode ($\nu = 3427\ cm^{-1}$) becomes the dissociation coordinate and is thus a disappearing mode, whilst the wavenumbers of the NH_2 deformation and the NH_2 twist ($\nu = 1623$ and $1455\ cm^{-1}$, respectively, in the ground state) are both arbitrarily reduced to $200\ cm^{-1}$. The transition state leading to C—H bond fission was treated similarly: the C—H asymmetric stretch vibration ($\nu = 2961\ cm^{-1}$) becomes the disappearing mode, and the wavenumbers of the CH_3 deformations (1485 and $1473\ cm^{-1}$ in the ground state) were dropped down to $200\ cm^{-1}$. The resulting calculated unimolecular decay rates, $k(E)$, are plotted in Fig. 9, as is the energy dependence of the ratio of these two rate constants. Clearly, in the limit of complete energy randomisation within the $CH_3NH_2^{\#}$ molecules prior to dissociation, RRKM theory would predict a dominant, though not exclusive, role for the C—H bond fission process.

Such a conclusion is at variance with the bulk of experimental observations regarding the UV photolysis of methylamine. The H-atom kinetic energy distributions we observe from photodissociation of CH_3NH_2 and CD_3NH_2 are very similar (recall Fig. 5), whilst the D atom yield from the latter is small. Similar comments apply for the D-atom kinetic energy distributions we observe from CH_3ND_2 and CD_3ND_2 photolysis. The earlier quantum yield estimates[9] ascribed *ca.* 75% of the total dissociation to N—H bond fission. None of these results are compatible with the predictions arising from the RRKM modelling outlined above. Indeed, if the premise of complete energy randomisation within the $CH_3NH_2^{\#}$ molecules prior to dissociation were valid then, on the basis of its endoergicity, we should expect the C—N bond fission process to make an, at least, comparable contribution to the total dissociation yield from these 'hot' ground state molecules, yet the quantum yield of process (4) has been estimated at <0.05.[9] Further, Waschewsky *et al.*[10] show the TKER spectrum associated with the ND_2 fragments resulting from 222.0 nm photolysis of CH_3ND_2 to peak away from zero, implying that these arise as a result of direct dissociation on the $\tilde{A}$ state surface, and not from unimolecular decay of hot $CH_3ND_2^{\#}$ molecules.

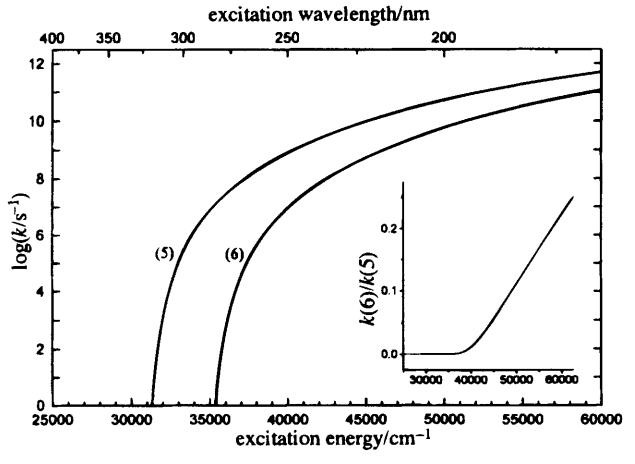

Fig. 9 Calculated unimolecular decay rates, $k(E)$, for the C—H and N—H bond fission channels assuming complete energy randomisation within the $CH_3NH_2^{\#}$ molecules prior to dissociation. Clearly, in the limit of complete energy randomisation, RRKM theory would predict a dominant, though not exclusive, role for the C—H bond fission process.

These observations, together with the recent *ab initio* work of Dunn and Morokuma,[5] suggest the following conclusions.

1. The major products of the photolysis of methylamine molecules following excitation to their first excited singlet state (the $\tilde{A}$ state) are H atoms together with CH_3NH fragments.

2. The TKER spectrum of the H + CH_3NH products is bimodal. This observation has been rationalised by assuming contributions to the total fragmentation yield from (*i*) a faster component associated with a rather 'direct' dissociation involving motion along the N—H dissociation coordinate on the $\tilde{A}$ state surface, coupling to the ground-state surface *via* the conical intersection in this exit channel, and ultimate dissociation to ground-state products and (*ii*) a slow component resulting from a 'statistical' dissociation of highly internally excited $CH_3NH_2^{\#}$ molecules arising as a result of internal conversion from the initially populated $\tilde{A}$ state. The relative importance of the 'slow' component appears to increase with decreasing excitation wavelength, probably because 'direct' dissociation to electronically excited $CH_3NH(\tilde{A})$ products becomes energetically allowed.

3. RRKM calculations presented here suggest that N—H bond fission should play at best a minor role in the dissociation of 'hot' $CH_3NH_2^{\#}$ molecules in which the energy is truly randomly distributed. Thus, as in our earlier work of CH_4 dissociation following excitation at 121.6 nm,[29] it appears that the dissociation of these 'hot' $CH_3NH_2^{\#}$ molecules leads to a democratic sampling of the phase space associated with one of the available fragmentation pathways (here the H + CH_3NH product channel) but not of the total available phase space. The present findings would suggest that IC to the ground state surface occurs not in the vertical Franck–Condon region, but only after the occurrence of some (irreversible) N—H bond extension, *i.e.* perhaps in the well associated with the $\tilde{A}/\tilde{X}$ conical section.

Clearly there still remains much to learn about the detailed dissociation dynamics of this molecule; experiments which attempt to look for infrared fluorescence from the $CH_3NH(\tilde{A})$ products predicted in this work might prove particularly profitable.

We are grateful to the EPSRC and NERC for equipment grants and the EPSRC for a studentship (to C.L.R.). It is also a pleasure to thank colleagues in Universität Bielefeld, Germany (Professor K. H. Welge and Dr. L. Schnieder) and in Bristol (Professor R. N. Dixon, Drs. A. J. Orr-Ewing, S. H. S. Wilson and C. M. Western and K. N. Rosser) for their many different, important contributions to this work. M.K. thanks the Japanese Society for the Promotion of Science for the award of a Postdoctoral Research Fellowship.

References

1 M. B. Robin, *Higher Excited States of Polyatomic Molecules, I*, Academic Press, New York, 1974.
2 M. Tsuboi, A. Y. Hirakawa and H. Kawashima, *J. Mol. Spectrosc.*, 1969, **29**, 216.
3 M-J. Hubin-Franskin, J. Delwiche, F. Tollet, M. Furlan and J. E. Collin, *J. Phys. B*, 1988, **21**, 189.
4 E. Kassab, J. T. Cleghorn and E. M. Evleth, *J. Am. Chem. Soc.*, 1983, **105**, 1746.
5 K. M. Dunn and K. Morokuma, *J. Phys. Chem.*, 1996, **100**, 123.
6 D. P. Taylor and E. R. Bernstein, *J. Chem. Phys.*, 1995, **103**, 10453.
7 S. W. Hwang, T. Higashihara, K. S. Shin and W. C. Gardiner Jr., *J. Phys. Chem.*, 1990, **94**, 2883.
8 S. W. Benson, *Thermochemical Kinetics*, Wiley, New York, 1968.
9 J. V. Michael and W. A. Noyes, *J. Am. Chem. Soc.*, 1963, **85**, 1228.

10 G. C. G. Waschewsky, D. C. Kitchen, P. W. Browning and L. J. Butler, *J. Phys. Chem.*, 1995, **99**, 2635.
11 R. J. Buenker, G. Olbrich, H-P. Schuchmann, B. L. Schurmann and C. von Sonntag, *J. Am. Chem. Soc.*, 1984, **106**, 4362.
12 S. Satyapal, J. Park, R. Bersohn and B. Katz, *J. Chem. Phys.*, 1989, **91**, 6873.
13 Y. Wen, J. Segall, M. Dulligan and C. Wittig, *J. Chem. Phys.*, 1994, **101**, 5665.
14 M. N. R. Ashfold, D. H. Mordaunt and S. H. S. Wilson, in *Adv. Photochem.*, 1996, **21**, 217 and references therein
15 J. S. Keller, P. W. Kash, E. Jensen and L. J. Butler, *J. Chem. Phys.*, 1992, **96**, 4324.
16 E. Jensen, J. S. Keller, G. C. G. Waschewsky, J. E. Stevens, R. L. Graham, K. F. Freed and L. J. Butler, *J. Chem. Phys.*, 1993, **98**, 2882.
17 S. H. S. Wilson, M. N. R. Ashfold and R. N. Dixon, *J. Chem. Phys.*, 1994, **101**, 7538.
18 S. B. Barone, A. A. Turnipseed, T. Gierczak and A. R. Ravishankara, *J. Phys. Chem.*, 1994, **98**, 11969.
19 R. Runau, S. D. Peyerimhoff and R. J. Buenker, *J. Mol. Spectrosc.*, 1977, **68**, 253.
20 M. N. R. Ashfold, C. L. Bennett and R. N. Dixon, *Chem. Phys.*, 1985, **93**, 293; *Faraday Discuss. Chem. Soc.*, 1986, **82**, 163.
21 L. D. Ziegler, *J. Chem. Phys.*, 1986, **84**, 6013; **86**, 1703.
22 M. I. McCarthy, P. Rosmus, H-J. Werner, P. Botschwina and V. Vaida, *J. Chem. Phys.*, 1987, **86**, 6693.
23 J. Biesner, L. Schnieder, J. Schmeer, G. Ahlers, X. Xie, K. H. Welge, M. N. R. Ashfold and R. N. Dixon, *J. Chem. Phys.*, 1988, **88**, 3607.
24 J. Biesner, L. Schnieder, G. Ahlers, X. Xie, K. H. Welge, M. N. R. Ashfold and R. N. Dixon, *J. Chem. Phys.*, 1989, **91**, 2901.
25 S. A. Henck, M. A. Mason, W-B. Yan, K. K. Lehmann and S. L. Coy, *J. Chem. Phys.*, 1995, **102**, 4772, 4783.
26 D. H. Mordaunt, M. N. R. Ashfold and R. N. Dixon, *J. Chem. Phys.*, 1996, **104**, 6460 and references therein.
27 D. H. Mordaunt, R. N. Dixon and M. N. R. Ashfold, *J. Chem. Phys.*, 1996, **104**, 6472.
28 G. P. Morley, I. R. Lambert, M. N. R. Ashfold, K. N. Rosser and C. M. Western, *J. Chem. Phys.*, 1992, **97**, 3157.
29 D. H. Mordaunt, I. R. Lambert, G. P. Morley, M. N. R. Ashfold, R. N. Dixon, C. M.Western, L. Schnieder and K. H. Welge, *J. Chem. Phys.*, 1993, **98**, 2054.
30 G. P. Morley, I. R. Lambert, D. H. Mordaunt, S. H. S. Wilson, M. N. R. Ashfold, R. N. Dixon and C. M. Western, *J. Chem. Soc., Faraday Trans.*, 1993, **89**, 3865.
31 J. Berkowitz, G. B. Ellison and D. Gutman, *J. Phys. Chem.*, 1994, **98**, 2744.
32 S. H. S. Wilson, J. D. Howe and M. N. R. Ashfold, *Mol. Phys.*, 1996, **88**, 841.
33 P. J. Robinson and K. A. Holbrook, *Unimolecular Reactions*, Wiley Interscience, New York, 1972.
34 J. M. Dyke, E. P. F. Lee and M. H. Zamanpour Niavaran, *Int. J. Mass Spectrom. Ion Processes*, 1989, **94**, 221.
35 F. Motte-Tollet, M-J. Hubin-Franskin and J. E. Collin, *J. Chem. Phys.*, 1992, **97**, 7314.
36 E. L. Woodbridge, M. N. R. Ashfold and S. R. Leone, *J. Chem. Phys.*, 1991, **94**, 4195.
37 I. W. M. Smith, *Kinetics and Dynamics of Elementary Gas Reactions*, Butterworths, London, 1980.

Paper 6/05420J; *Received* 2nd *August*, 1996